energy&fuels

pubs.acs.org/EF

Article

Modeling Formic Acid Combustion

Fekadu Mosisa Wako, Gianmaria Pio,* and Ernesto Salzano

Cite This: *Energy Fuels* 2022, 36, 14382−14392

Read Online

ACCESS | Metrics & More | Article Recommendations | Supporting Information

ABSTRACT: Nowadays, the knowledge of the gas-phase chemistry of formic acid is paramount for several industrial sectors, including energy supply and the production of bulk chemicals. In this work, a simplified kinetic mechanism and a detailed kinetic mechanism deriving from a rate-based selection algorithm were developed and tested against experimental data available in the literature. The former contains 141 species and 453 reactions, whereas the latter comprises 90 species and 1047 reactions. A focus on a low initial temperature (i.e., up to 500 K) was provided by comparing the numerical estimations with laminar burning velocity and jet-stirred measurements at several conditions. A good agreement among numerical predictions and experimental data was observed, especially for the simplified kinetic mechanism. The accuracy of the generated mechanism allowed for further analysis of the chemistry of the system, enlightening some determining aspects of the chemistry of formic acid. The produced mechanism can be also intended as per seed mechanism for the generation of kinetic models focused on the chemistry of biofuels. Indeed, the characterization of chemical aspects of formic acid occurring in an oxidative environment is crucial due to its relevance as an energy vector as well as an intermediate compound in the decomposition of larger hydrocarbons and bio-oils.

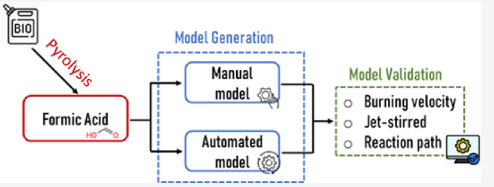

1. INTRODUCTION

Organic acids are one of the main pollutants in the atmosphere that leads to the formation of acid rain.[1,2] Currently, this class of compounds can derive from the emission of exhaust gas from internal combustion engines[3,4] or wildfire,[5] thus involving both urban and rural atmospheres.[1] Among organic acids, monocarboxylic acids have been largely detected within exhaust gas.[4,6,7] In particular, formic acid (HOCHO) is an intermediate product during the oxidation of oxygenated biofuels[8] such as methanol,[9] ethyl acetate,[10] and dimethyl ether.[11] In addition, HOCHO is mainly obtained from cellulose pyrolysis through ring opening and fragmentation reactions of levoglucosan (i.e., the main intermediate product of cellulose pyrolysis) and 1,6-anhydroglucofuranose in the temperature range of 400−500 and 300−400 °C, respectively.[12] As a result, the chemistry of formic acid plays a determining role in the sustainable production of energy from several oxygenated species being included in several kinetic models.[13−15]

From a chemical perspective, the interest in industrial processes directly producing formic acid from carbon dioxide has been largely increased as they can be considered for the carbon capture, utilization, and storage (CCUS) as well as for the production of hydrogen carrier component through the reaction $CO_2 + H_2 \leftrightharpoons$ HOCHO.[16] One liter of formic acid can have the same amount of hydrogen as in a compressed hydrogen storage tank at 700 bar.[17] On the other hand, it contains 53 g l^{-1} hydrogen at room temperature and atmospheric pressure, which is twice as much as compressed hydrogen gas can attain at typical storage conditions.[18] Thermodynamically, dehydrogenation of formic acid has a low reaction enthalpy, which leads to hydrogen production at a lower temperature (lower than 100 °C).[18] Since the number of C−C bonds in a fuel structure is related to soot formation tendency,[19] the lack of C−C bonds in the chemical structure of formic acid, coupled with its high energy density, can favor its application within fuel blends in advanced engine technology.[19]

The chemistry of formic acid has been investigated either experimentally in terms of laminar premixed flames[20] or numerically by kinetic models.[15] Yin et al.[21] reported experimental and kinetic studies of formic acid laminar flame speeds over a wide equivalence ratio range and a temperature range of 423−453 K. The authors used the Glarborg and Updated AramcoMech2.0 kinetic models as per comparison with their experimental data, the former well agreed with the experimental results, whereas the latter overestimated the laminar burning velocity data. More recently, Osipova et al.[22] conducted an experimental and numerical study on the laminar burning velocity of pure formic acid and formic acid/hydrogen mixtures at temperatures of 368, 373, and 423 K and an equivalence ratio ranging from 0.5 to 1.5. From the comparison of the model and experimental data, the authors strongly suggest the importance of improving the existing kinetic models or generating a new detailed kinetic model. Nevertheless, a dearth of specific studies dedicated to the kinetic mechanisms of formic acid can be observed in the current literature. On the other hand,

Received: September 28, 2022
Revised: November 2, 2022
Published: November 15, 2022

https://doi.org/10.1021/acs.energyfuels.2c03249
Energy Fuels 2022, 36, 14382−14392

formic acid oxidation in a static thermal reactor within a temperature range of 613−743 K has been reported by Bone and Gardner.[23] From the study, the pressure increase after formic acid oxidation is relatively slow, indicating low reactivity. Several studies[11,13,15] have reported the formation and consumption of formic acid, among which the study reported by Battin-Leclerc et al.[15] revealed the formation of formic acid in hydrocarbon flames to be primarily by the addition of OH radicals to formaldehyde followed by elimination of a hydrogen atom[15] through the reactions $CH_2O + OH (+ M) \leftrightarrow HOCH_2O (+ M)$ and $HOCH_2O (+ M) \leftrightarrow HOCHO + H (+ M)$. Similarly, the study reported by Taylor et al.[24] on the formation of formic acid revealed the formation of formic acid by the reaction between OH and acetylene.

In addition, the theoretical kinetic study of the unimolecular decomposition of formic acid via high-level quantum chemistry calculation has been reported by Chang et al.[25] The gas-phase reaction between HOCHO and hydroxyl radical with the high-level quantum mechanical theory has been studied by Anglada.[26] In the same way, the reaction of intermediate radical HOCO with HO_2 has been studied by Yu et al.[27] employing quadratic configuration interaction with the single- and double-excitations (QCISD(T)) method with a large basis set on the singlet and triplet potential energy surfaces. Later on, Marshall and Glarborg[28] developed the first detailed chemical kinetic model for formic acid oxidation. The model has shown a good agreement with a Bunsen burner laminar flame speed data from de Wilde and van Tiggelen[29] for equivalence ratios ranging from 0.4 to 1.3. Rate coefficients for the reactions HOCHO + H, HOCHO + O, and HOCHO + HO_2 were obtained from ab initio calculations. The study also concluded the HOCHO + OH ↔ OCHO + H_2O reaction as the main consumption pathway for formic acid where OCHO further dissociates producing CO_2 + H and HOCO. Recently, Sarathy et al.[17] reported a detailed chemical kinetic mechanism called Updated Aramco2.0 using the AramcoMech2.0 kinetic model[30] as a base mechanism. The authors validated the updated mechanism with the experimental laminar burning velocity data of pure formic acid and its mixtures with H_2 and CO_2. Apart from these two detailed kinetic models, there are limited comprehensive kinetic mechanisms available in the literature.

For these reasons, this study is devoted to the development of detailed kinetic mechanisms for formic acid combustion. Two alternative strategies for the generation of kinetic mechanisms will be implemented and compared. The accuracy of the developed models will be tested against experimental data and compared with numerical estimations from the literature. Eventually, further insights into the chemistry ruling the decomposition of formic acid in an oxidative environment will be provided.

2. NUMERICAL METHODS

In this work, different strategies for the generation of kinetic mechanisms were adopted and tested. Hence, a specific subsection dedicated to each strategy is reported below: upgrading the existing mechanism and generating a detailed kinetic model with the help of dedicated software, i.e., Reaction Mechanism Generator (RMG).

2.1. Upgrade of the Existing Mechanism. An existing detailed kinetic mechanism developed at the University of Bologna (KiBo) was used as a seed mechanism for $C_0−C_3$ chemistry because of its elevated accuracy in predicting the chemistry of short-chain hydrocarbons.[31] The mechanism was enlarged to include the chemistry, thermodynamic properties, and transport coefficients of oxygenated species including formic acid. In this work, the chemistry of formic acid in an oxidative environment was added by manually collecting and incorporating unimolecular decomposition and hydrogen abstraction (via H, OH, HO_2, O, and O_2) reactions as well as radical consumption reactions of its major intermediate products (i.e., HOCO and OCHO). The updated version of the mechanism is referred to as manually updated KiBo, KiBo_MU. Primarily, the rate coefficients of these reactions were taken from experimental data reported in the literature and/or high-level quantum chemistry calculations, when available. Alternatively, rate coefficients obtained by correlations and estimation procedures (e.g., the reaction family approach) were considered. For the species added during the implementation of the described procedure, thermodynamic data were taken from the following databases: PrimaryThermoLibrary,[32] DFT_QCI_thermo,[33] CHO,[34] and CBS_QB3_1dHR,[35] following the same concept of prioritization mentioned before, i.e., data generated through ab initio calculations at a high level of theory were added, when possible.

2.2. Generation of a New Detailed Kinetic Mechanism. In this case, a detailed kinetic mechanism named KiBo_AG was developed using RMG, which is an open-source rate-based automatic kinetic mechanism generation software.[36,37] The construction of the mechanism starts with specifying a range of initial conditions of interest such as temperature, pressure, fuel composition, kinetic and thermodynamic libraries, and termination criteria. Then, an iterative procedure using a rate-based algorithm is employed for the selection of species and reactions to be added to the generating core mechanism until termination criteria (e.g., time or conversion of a given reactant) are satisfied.[38] Within the generation procedure, core and edge mechanisms are generated. Species are allocated in the proper mechanism based on their net rate of production in comparison with user-defined tolerances: *Move to Core* (= 0.012), *Keep in Edge* (= 0.01), and *Interrupt Simulation* (= 0.02). Once the simulation converged, the resulting core mechanism can be refined by the identification of the most influential species and reaction, thanks to the so-called sensitivity analysis, followed by an additional iteration in RMG with updated libraries.

The mechanism was generated at the following conditions: temperature 400−2000 K, pressure 1−100 bar, stoichiometric composition, and termination criteria of 50 s or fuel conversion equal to 0.99. The abovementioned boundary conditions were posed, given preliminary investigations and previous studies conducted by the same research group.[37] Indeed, it has been demonstrated that the implementation of a stoichiometric composition, termination criteria larger than 40 s, temperature up to 2000 K, and pressure up to 100 bar in RMG are sufficient to include the most relevant pathways for operative conditions representative of combustion processes. This approach leads to a considerable reduction of the computational costs required for the generation of a kinetic mechanism with little impact on the quality of the output.[37] The necessary thermodynamic data were taken from PrimaryThermoLibrary,[32] DFT_QCI_thermo,[33] thermo_DFT_CCSDTF12_BAC,[39] CBS_QB3_1dHR,[35] CHO,[34] and FFCM1(−),[40] whereas BurkeH2O2inN2,[41] Klippenstein_Glarborg2016,[42] and C2H4 + O_Klipp2017[43] were used as kinetic libraries. Please consider that the cited databases are reported with the nomenclature adopted by the RMG repository to facilitate their individuation. In all cases, sources were prioritized in the presented order based on the accuracy of the theory of the quantum chemistry calculation involved. RMG uses group additivity and rates family methods to estimate the thermochemical and kinetic data of species whose data is not present in the listed library.[44] Nevertheless, these methods are not accurate enough to correctly estimate data for oxygenated species,[45] suggesting the use of more robust theories, such as ab initio calculations. This kind of quantum mechanical calculation is the most trustworthy because they apply various mathematical transformations and approximations to find optimal molecular geometry, vibrational frequencies, and bond energies.[45] For these reasons, a sensitivity analysis was performed to identify species and reactions significantly affecting the generated mechanism; namely, a threshold value of 0.03 for the normalized sensitivity coefficient was considered. The source used for the thermodynamic or kinetic parameters for the selected species was replaced with values deriving

https://doi.org/10.1021/acs.energyfuels.2c03249
Energy Fuels 2022, 36, 14382−14392

from ab initio calculations from the literature, if available. The resulting mechanism was tested, as described in the following sections. The procedure described in this paragraph is sketched in Figure 1.

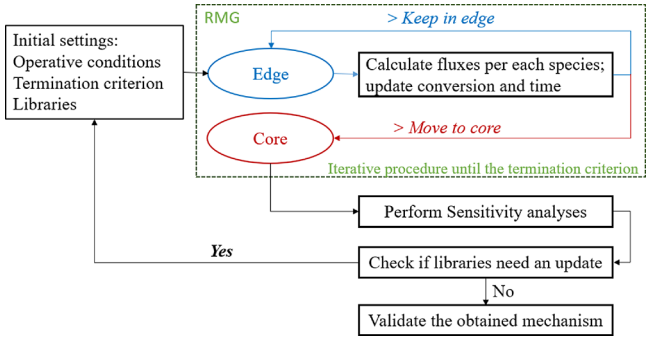

Figure 1. Schematic representation of the procedure adopted for developing a detailed chemical kinetic mechanism using RMG.

2.3. Mechanism Validation. The two kinetic mechanisms were tested against the laminar burning velocity and jet-stirred data of formic acid oxidation available in the literature. In addition, additional mechanisms from the literature were tested for the sake of comparison. More specifically, models produced by Marshall and Glarborg[28] and Updated AramcoMech2.0[17] were considered at this stage.

Details of kinetic mechanisms available in the literature and the mechanisms developed in this study are shown in Table 1.

Table 1. Kinetic Mechanisms Applied in This Study

no.	mechanisms	no. of species	no. of reactions	ref
1	Marshall and Glarborg	27	75	28
2	Updated AramcoMech2.0	305	1761	17
3	KiBo_MU	141	453	this work
4	KiBo_AG	90	1047	this work

All the simulations were performed using an open-source Cantera suite[46] with appropriate reactor modules using a transient condition as a first-attempt solution for the steady-state conditions. The following simulation criteria were used for solving steady-state (ss) and transient state (ts) problems: absolute tolerance_ss = 1.0×10^{-9}, relative tolerance_ss = 1.0×10^{-14}, absolute tolerance_ts = 1.0×10^{-5}, and relative tolerance_ts = 1.0×10^{-14}. An adaptive grid was determined by using the following criteria: maximum acceptable ratio among adjacent solutions (ratio) equal to 3, maximum first derivative for adjacent solutions (slope) equal to 0.06, and maximum acceptable second derivative for adjacent solutions (curve) equal to 0.12, following the recommendations reported in the current literature.[47] The Soret effect and multicomponent transport model were neglected, at first, to generate a first-guess result and subsequently accounted for the final solution. Comparison between the experimental and simulation results of laminar burning velocity and jet-stirred data by the two kinetic mechanisms at different reaction conditions was performed based on the availability of experimental data from the current literature. The laminar burning velocity was estimated, assuming a monodimensional, adiabatic reactor running in a steady-state mode fed by a premixed gaseous stream. Conversely, the response of formic acid consumption and combustion product formation to initial temperature and residence time was simulated in an ideal continuously stirred tank reactor called a jet-stirred reactor. In this case, the temperature was investigated within the range of 500−1100 K, whereas the residence time was set to be 2 s. Furthermore, with the help of sensitivity analysis, key reactions for formic acid combustion were evaluated under different fuel compositions. Likewise, the main consumption pathways of formic acid decomposition and intermediate radical transformations were assessed with the aid of a reaction path analyzer. To this aim, a global[48] pathway algorithm that decoupled the timescale and the perturbation was implemented for the identification of the relevant fluxes.[49] The range of reaction conditions used in this study is shown in Table 2.

Table 2. Ranges of Reaction Conditions Considered for the Simulation of Laminar Burning Velocity and Jet-Stirred Reactors

investigated parameter	temperature (K)	fuel mixtures	equivalence ratio
laminar burning velocity	368−453	HOCHO/O_2/(Ar/N_2)	0.5−1.6
jet-stirred reactors	550−1100	HOCHO/O_2/He	0.5, 1, 2
sensitivity analysis	423; 453	HOCHO/Ar	0.8, 1.0, 1.5
flux diagram	900	HOCHO/Ar	1.0

3. RESULTS AND DISCUSSION

In this section, the main findings are presented and discussed, given experimental measurements from the current literature, when available. Considering the different nature of the data analyzed, specific subsections were dedicated to the laminar burning velocity, jet-stirred reactor data, sensitivity analysis, and flux analysis.

3.1. Laminar Burning Velocity. The laminar burning velocity of formic acid/air mixtures at different initial temperatures over a wide range of equivalence ratios was numerically studied. The simulation results with their corresponding experimental measurements from the literature are shown in Figures 2−4. More specifically, Figure 2 depicts the laminar burning velocity of HOCHO/air mixtures at reaction temperatures of 373 and 423 K, whereas Figure 3 reports HOCHO/O_2/N_2 at 433 and 453 K, and Figure 4 shows data for HOCHO/O_2/Ar at 368 K. In addition, the laminar burning velocity of mixtures containing HOCHO and CH_4 in the air was also reported (Figure 5).

As can be seen from Figure 2a,b, under the investigated conditions, KiBo_MU and KiBo_AG kinetic models are in good agreement with the experimental results. The laminar burning velocity increases with increasing equivalence ratio and reaches its peak value at a fuel-to-air ratio of 1.1 using all the investigated kinetic mechanisms, which are also true in the case of experimental data from Sarathy et al.[17] The equivalence ratio where the fundamental laminar burning velocity is observed is in line with most hydrocarbons, as it is related to the compositions showing the maximum adiabatic temperature and maximum concentration of H radicals.[51] Under the same condition, an increase in temperature by 50 K (i.e., 373−423 K) increases the maximum laminar burning velocity by 8 cm/s (i.e., 22−30 cm/s) in the case of the experiment and by 7 cm/s using KiBo_MU and KiBo_AG. In addition, the models were compared with the existing formic acid kinetic models and found to show a better agreement. However, discrepancies were observed in rich flames for Glarborg, whereas the Updated Aramco2.0 kinetic model fairly agreed with the measured burning velocity.

On the other hand, as can be seen from Figure 3a,b at 433 and 453 K, respectively, KiBo_MU and KiBo_AG apparently predicted the laminar burning velocities well and the results satisfactorily agreed with the experimental results from de Wilde and van Tiggelen[29] and Yin et al.[21] Given the limited equivalence ratio considered in the case of 433 K temperature, at both 433 and 453 K, the numerical and experimental value of maximum laminar burning velocity was found to be obtained at an equivalence ratio of 0.9, which might be due to the increased

https://doi.org/10.1021/acs.energyfuels.2c03249
Energy Fuels 2022, 36, 14382−14392

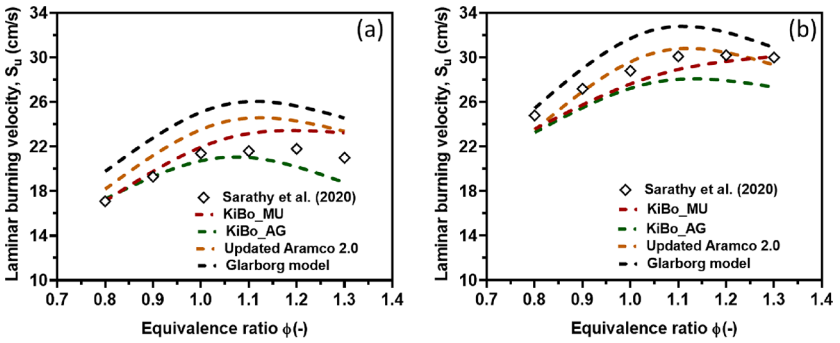

Figure 2. Laminar burning velocity for HOCHO/air mixtures at 373 K (a) and 423 K (b). The symbols mark the experimental data from Sarathy et al.,[17] while the broken lines denote the model predictions.

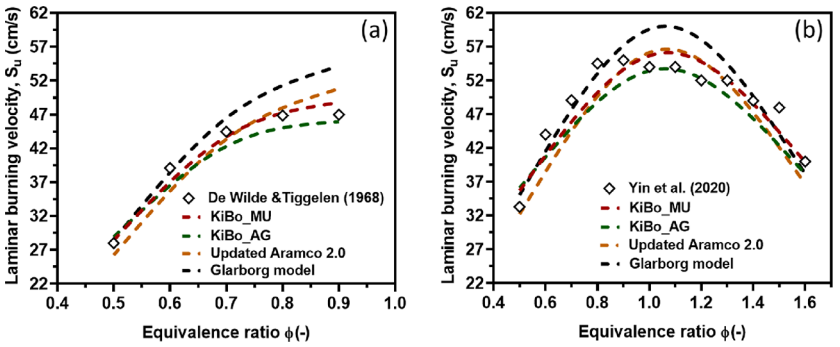

Figure 3. Laminar burning velocity for HOCHO/O_2/N_2 mixtures at 433 K (a) and 453 K (b); 35% O_2, 65% N_2. The symbols mark the experimental data for 433 K from de Wilde and van Tiggelen[29] and 453 K from Yin et al.,[21] while the broken lines denote the model predictions.

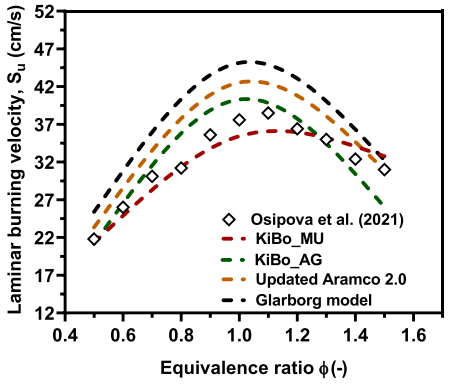

Figure 4. Laminar burning velocity for HOCHO/O_2/Ar blends at 368 K; the mole fraction of Ar is 0.55. The symbols mark the experimental data from Osipova et al.,[50] while the broken lines denote the model predictions.

oxygen composition in the fuel mixture. The increase in 20 K (i.e., 433−453 K) increases the laminar burning velocity by 8 cm/s, which is equivalent to a 50 K increase (i.e., 373−423 K), as shown in Figure 2a,b. From this, it can be said that the increase in oxygen composition in the fuel mixture increases the burning rate more than the increase in temperature, leading to peak laminar burning velocity happening in a lean condition. Moreover, as can be seen from Figure 3b, the Glarborg model showed large discrepancies in laminar burning velocity, particularly at rich composition, which could be associated with the rate coefficient of the CO + OH ↔ CO_2 + H reaction, which is one of the key reactions for the formic acid. This reaction was incorporated as a pressure-dependent reaction in the Glarborg model but as an Arrhenius-like reaction in KiBo_MU. In the latter case, coefficients were taken from the ab initio calculations reported by Joshi and Wang.[52] Thus, the better accuracy observed in KiBo_MU at this particular

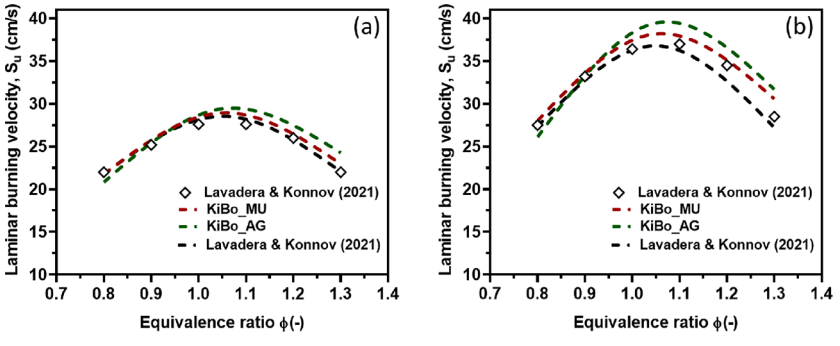

Figure 5. Laminar burning velocities of (0.75 HOCHO + 0.25 CH4) + air flames (a) and (0.5 HOCHO + 0.5 CH4) + air flames (b) at 353 K.

https://doi.org/10.1021/acs.energyfuels.2c03249
Energy Fuels 2022, 36, 14382−14392

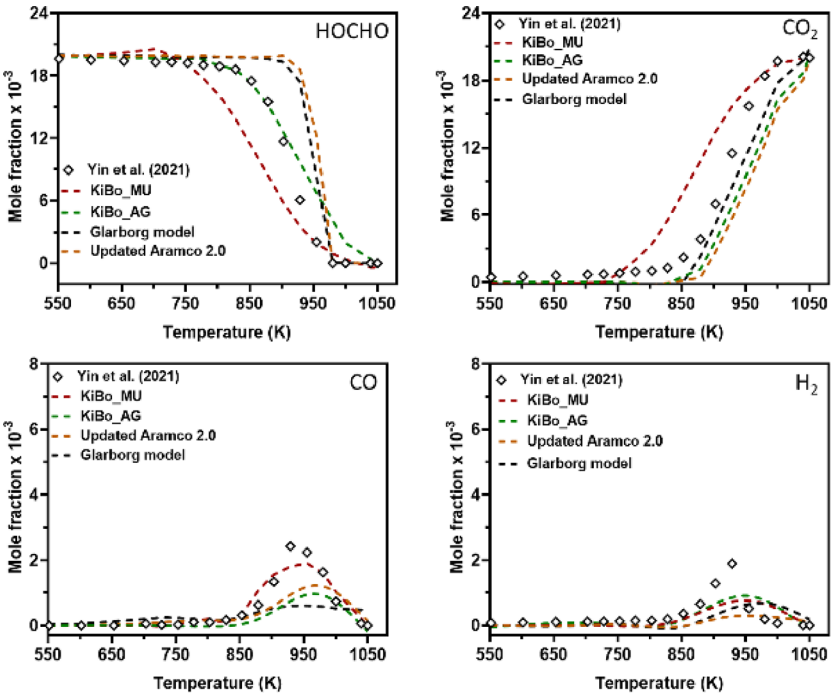

Figure 6. Mole fraction profiles of HOCHO, CO_2, CO, and H_2 at temperatures of 500−1100 K, an equivalence ratio of 0.5, atmospheric pressure, and a residence time of 2 s. Symbols, experimental data from Yin et al.;[54] broken lines, simulation results.

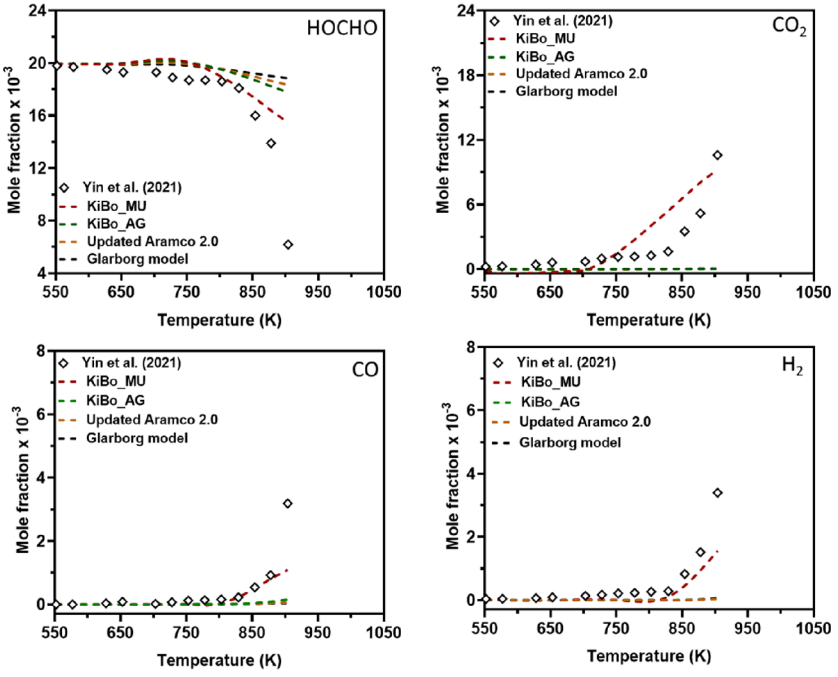

Figure 7. Mole fraction profiles of HOCHO, CO_2, CO, and H_2 at temperatures of 500−1100 K, an equivalence ratio of 1.0, atmospheric pressure, and a residence time of 2 s. Symbols, experimental data from Yin et al.;[54] broken lines, simulation results.

condition may be due to the difference in the rate coefficient of the aforementioned reaction.

The laminar burning velocity of HOCHO/Ar mixtures at a reaction temperature of 368 K, atmospheric pressure, and an equivalence ratio ranging from 0.5 to 1.5 is shown in Figure 4. In the same way, the current kinetic models well mimicked the experimental laminar burning velocity and comparably showed better agreement than the existing kinetic models. Furthermore, as can be seen from Figure 5a,b, the laminar burning velocity of fuel mixtures (i.e., HOCHO/CH_4/air mixture) has been studied in the equivalence ratio range of 0.8−1.3 and an initial temperature of 353 K. Methane addition was found to increase the reaction rate and apparently favor laminar burning velocity. It is worth noting from the figure that when the equivalence ratios are 1.0 and 1.1, the laminar burning velocity is not affected regardless of the methane composition in the fuel mixture. From this, it can be seen that the maximum reactivity of the fuel mixture is achieved at these equivalence ratios, as is the

https://doi.org/10.1021/acs.energyfuels.2c03249
Energy Fuels 2022, 36, 14382−14392

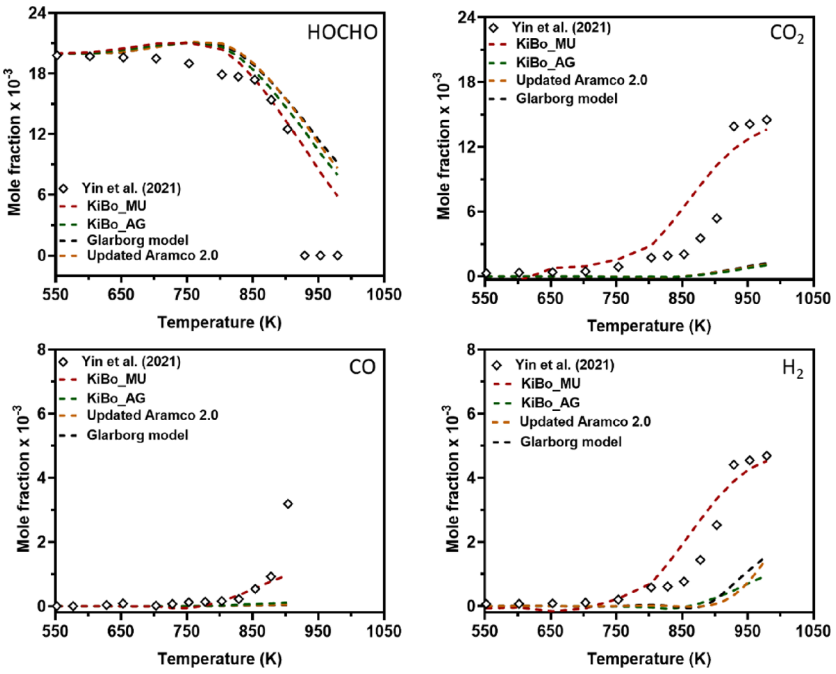

Figure 8. Mole fraction profiles of HOCHO, CO_2, CO, and H_2 at temperatures of 500−1100 K, an equivalence ratio of 2.0, atmospheric pressure, and a residence time of 2 s. Symbols, experimental data from Yin et al.;[54] broken lines, simulation results.

maximum laminar burning velocity. From both figures, the laminar burning velocity result from this study using KiBo_MU and KiBo_AG is in good agreement with the experimental data reported by Lavadera and Konnov[53] and the model result obtained by the same author. Overall, under the investigated conditions, KiBo_MU and KiBo_AG reasonably predicted the burning velocity and showed better accuracy than the existing kinetic models at low temperatures. Further considerations on these aspects will be provided in the following sections where the accuracy of the selected mechanisms will be tested against experimental data at high temperatures derived by jet-stirred reactors.

3.2. Profiles of Main Products. The species profiles from the jet-stirred reactor (JSR) reported by Yin et al.[54] at a temperature range of 600−1100 K, atmospheric pressure, a residence time of 2 s, and an equivalence ratio ranging from 0.5 to 2.0 were considered for validation. The numerical results obtained in this work along with the experimental measurements from a recent study reported by Yin et al.[54] are shown in Figures 6−.

Regardless of the investigated composition, numerical models show that formic acid does not autoignite at intermediate temperatures, as also observed at higher pressures.[55] From the thermal decomposition of HOCHO at intermediate temperatures, the active onset decomposition temperature and complete consumption of HOCHO are found to be at 803 and 1050 K, respectively. From the simulation result using KiBo_MU at lean conditions, around 42% of HOCHO was consumed at 903 K and 36% consumed within a temperature range of 929−955 K, whereas 14 and 50% of HOCHO were consumed, respectively, at 903 and 929−955 K in the case of KiBo_AG. From the experimental result reported by Yin et al.,[54] 30% of HOCHO was consumed at 903 K, while 31% was consumed within a temperature range of 929−955 K. Similarly, at stoichiometric composition, more than 95% of HOCHO get consumed within a temperature range of 878−903 K using KiBo_MU and KiBo_AG, where around 70% of HOCHO decomposed, according to the experimental result from Yin et al.[54] under the same temperature range. In rich flames, with KiBo_MU, 1/3 of HOCHO gets consumed within a temperature range of 803−903 K, and the remaining consumption happened between 929 and 979 K, while with KiBo_AG, 1/10 gets consumed within a temperature range of 803−903 K, and the remaining between 929 and 979 K. A possible explanation for the difference in KiBo_MU and KiBo_AG in predicting the decomposition of formic acid might be due to the difference in reaction branches included in each mechanism as well as in rate coefficients associated with the reactions HOCHO + O ↔ HOCO + OH, HOCHO + O ↔ OCHO + OH, and 2 HOCO ↔ CO_2 + HOCHO, which are only incorporated in KiBo_AG, and the rate coefficients derive from estimations. In this sense, additional elements and insights on the chemistry of formic acid and the developed mechanisms will be provided in the following section.

The decarboxylation reaction (i.e., HOCHO ↔ CO_2 + H_2) and hydrogen abstraction reactions by HO_2 (i.e., HOCHO + HO_2 ↔ HOCO + H_2O_2 and HOCHO + HO_2 ↔ OCHO + H_2O_2), OCHO ↔ CO_2 + H, and abstraction reaction of hydroxycarboxyl radical by O_2 (i.e., HOCO + O_2 ↔ CO_2 + H_2O_2) are found to be the key reactions affecting the decomposition of HOCHO under the probed condition. Even though the rate coefficients of these reactions were taken from ab initio, it seems that they have to be revised for better agreement of the HOCHO consumption and production of combustion products. The current models' results are also compared with the recently reported formic acid mechanism from the Saudi Aramco research group (Updated Aramco2.0) and the first formic acid kinetic model (i.e., the Glarborg kinetic model). The rate coefficients of the HOCHO + H ↔ HOCO + H_2 and HOCHO + HO_2 ↔ HOCO + H_2O_2 reactions were multiplied by a factor of 2 in this study to predict well the formic acid decomposition in the jet-stirred reactor. Similarly, in the Updated Aramco2.0 model, the rate coefficients of the two reactions were multiplied by a factor of 2. The better

https://doi.org/10.1021/acs.energyfuels.2c03249
Energy Fuels 2022, 36, 14382−14392

predictability observed in KiBo_MU could be associated with the OCHO ↔ CO_2 + H reaction, which is not incorporated in Updated Aramco2.0, and rate coefficients of the HOCHO + O ↔ HOCO + OH and HOCHO + O ↔ OCHO + OH reactions, in which it was multiplied by a factor of 2 in the case of Updated Aramco2.0. Overall, KiBo_MU showed better agreement for all species; however, KiBo_AG showed some variation, especially for CO_2 and H_2. Comparably, our models capture fairly the experimental observations than Updated Aramco2.0 and Glarborg kinetic models.

3.3. Chemistry of Formic Acid. Considering the quality in mimicking either low- or high-temperature data shown by KiBo_MU and KiBo_AG, a focus on the chemistry of the systems is provided for these mechanisms only. In particular, flux diagrams and sensitivity analyses were performed in different conditions representative of the system.

As can be seen from the species profile study reported in the previous section, most of the formic acid is consumed in the temperature range of 878−900 K. From this perspective, to better realize the decomposition of HOCHO at this particular condition and gain insight into its combustion kinetics, flux analysis was performed using KiBo_MU and KiBo_AG at the stoichiometric condition and 900 K, as shown in Figures 9 and

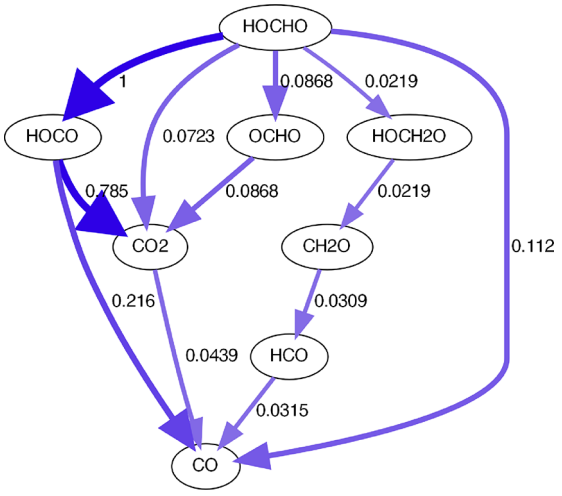

Figure 9. Reaction path diagram for oxidation of HOCHO at 900 K and stoichiometric condition using KiBo_MU.

10. Clearly, under the conditions studied, HOCHO is consumed by hydrogen abstraction reactions and two unimolecular decomposition reactions forming CO and H_2O, CO_2 and H_2. It was observed from the flux analysis that the formation of HOCO via the H-abstraction reaction (i.e., via H, OH, and HO_2) represents the dominant pathway for HOCHO consumption, rather than the OCHO formation pathway that decomposes to CO_2 + H. Likewise, cleavage of the C−O bond in HOCO was found to be the main pathway leading to CO_2 + H than the OCHO cleavage. Thus, HOCO + O_2 ↔ CO_2 + HO_2 is the most dominant pathway for the consumption of HOCO, which is in line with the study reported by Yin et al.[54] In addition, in the case of KiBo_AG (Figure 10), thermal decomposition of HOCO to OCHO followed by further dissociation leading to CO_2 + H via OCHO ↔ CO_2 + H is found to be a key pathway in the fuel combustion execution. Furthermore, by reacting with H through $HOCH_2O$ ↔ HOCHO + H, formic acid formed back the $HOCH_2O$ radical,

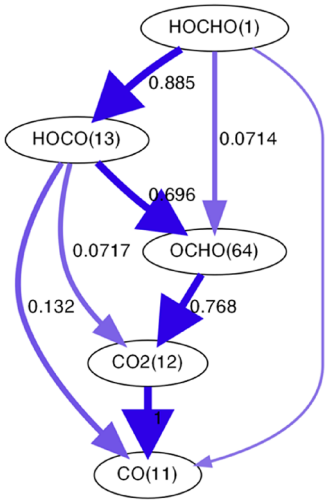

Figure 10. Reaction path diagram for oxidation of HOCHO at 900 K and stoichiometric condition using KiBo_AG.

which further decomposes to CH_2O + OH, as shown in Figure 9. Similarly, formaldehyde with O_2 forms HCO, in which further decomposition of HCO gives CO and H. This pathway of forming alkoxy radical was not reported in recent flux analysis studies and was only observed when KiBo_MU is used. It is worth mentioning that the direct production of CO_2 is negligible under the investigated conditions, according to KiBo_AG. Overall, the dissimilarity in reaction path analysis observed between KiBo_MU and KiBo_AG could be related to the adopted methodology for mechanism generation.

The most influential reactions at lean, stoichiometric, and rich conditions during formic acid oxidation were analyzed through sensitivity analysis using KiBo_MU and KiBo_AG kinetic models. Recent formic acid combustion studies have reported sensitivity analysis at different initial temperatures and fuel compositions. For instance, Marshal and Glarborg reported a list of sensible reactions in lean flame and at a temperature of 433 K.[28] Sarathy et al.[17] investigated sensitivity analysis at 373 K and stoichiometric composition. Similarly, Yin et al.[21] analyzed sensitivity analysis at 453 K under lean and rich conditions. The kinetic parameters associated with the majority of reactions highlighted by the cited literature are derived from accurate sources in the case of the mechanisms developed in this work. Hence, alternative conditions of interest were investigated. More specifically, this work presents sensitivity analysis at initial temperatures of 423 and 453 K and in all flame conditions (i.e., lean, stoichiometric, and rich conditions). The sensitivity results at the aforementioned temperature, atmospheric pressure, and equivalence ratios of 0.8, 1.0, and 1.5 are shown in Figures 11 and 12. The effects of hydrogen reactions such as H + O_2 ↔ O + OH, H + O_2 ↔ 2 OH, H_2 + O_2 ↔ H + HO_2, H + OH + M ↔ H_2O + M, H + O_2 (+ M) ↔ HO_2 (+ M), and H + HO_2 ↔ H_2 + O_2 on the laminar burning velocity of formic acid are not shown here as they are widely studied.[17,21,53]

The H-abstraction reaction of HOCHO by OH has a positive sensitivity coefficient on fuel oxidation at all conditions due to the rapid dissociation of the produced radical forming CO_2 and H. However, the reaction has a negligible impact on rich flames, according to KiBo_AG. Conversely, the automatically generated mechanism appears to be largely affected by the kinetics of the H-abstraction by H. Although the chain termination of HOCO by H, OH, and O_2 showed strong negative sensitivity coefficients

https://doi.org/10.1021/acs.energyfuels.2c03249
Energy Fuels 2022, 36, 14382−14392

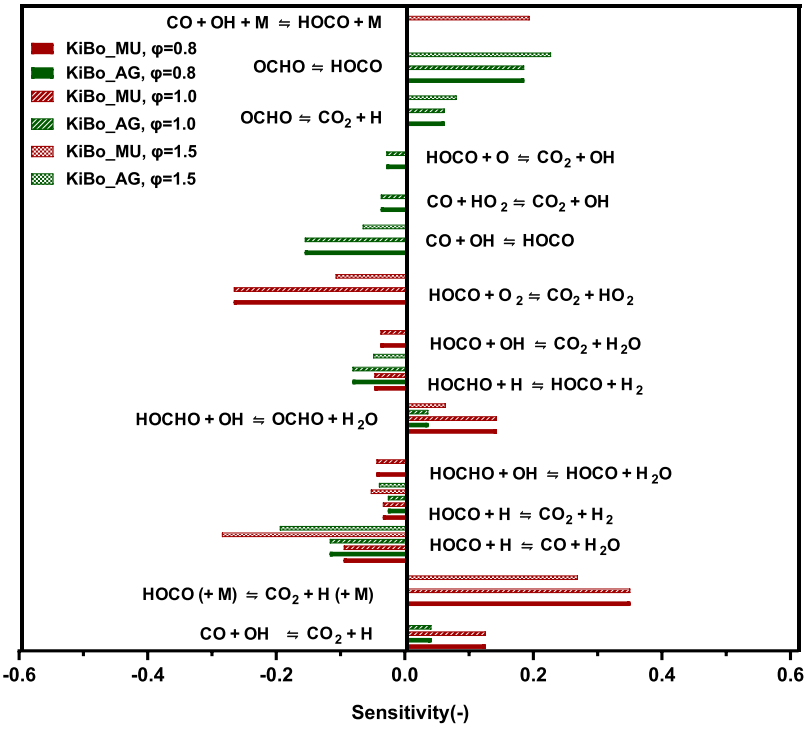

Figure 11. Sensitivity coefficients for laminar burning velocity in the oxidation of HOCHO/air flames, T = 423 K, φ = 0.8, 1.0, and 1.5 using KiBo_MU and KiBo_AG.

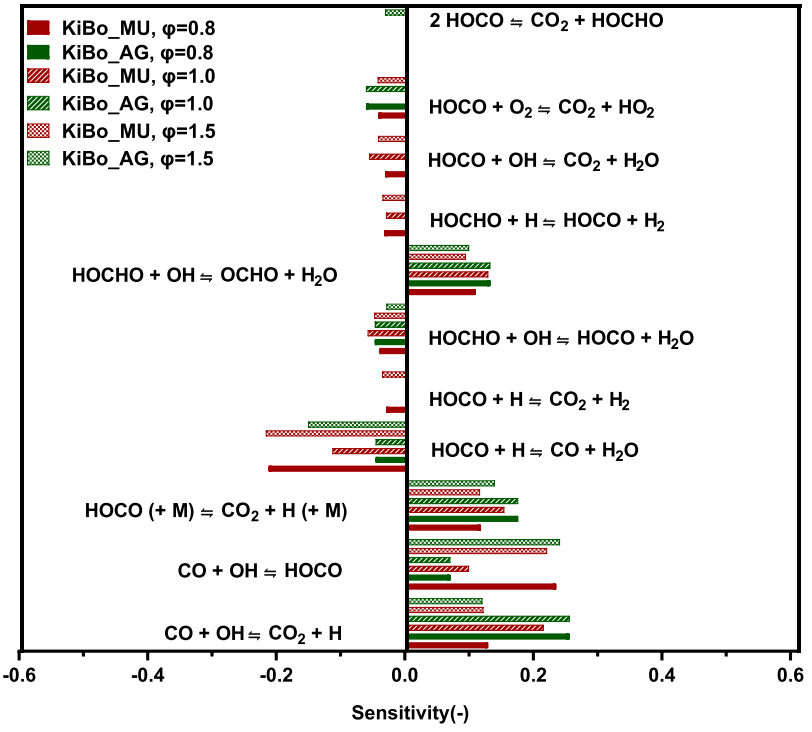

Figure 12. Sensitivity coefficients for laminar burning velocity in the oxidation of HOCHO/O_2/N_2, 35% O_2, 65% N_2, T = 453 K, φ = 0.8, 1.0, and 1.5 using KiBo_MU and KiBo_AG.

for both mechanisms, the unimolecular decomposition to CO_2 and H was considered as an impacting reaction by the KiBo_MU, exclusively. On the one hand, the observed discrepancies reveal that the alternative strategies adopted for the generation of detailed kinetic mechanisms implicitly bring to the attention different reactions. However, on the other hand, it is worth noting that kinetic coefficients related to the mentioned reactions derive from a calculation performed at a high level of theory. Hence, the robustness of the adopted databases was demonstrated.

Furthermore, as can be seen from Figure 12, for an initial temperature of 453 K, using the two kinetic models, radical

https://doi.org/10.1021/acs.energyfuels.2c03249
Energy Fuels 2022, 36, 14382−14392

Table 3. Radical Consumption Reactions, Sources, and Kinetic Coefficients during Formic Acid Oxidation, as Included in the Investigated Mechanisms[c]

reactions	mechanism	A	n	E_a	sources
OCHO ↔ CO_2 + H	KiBo_MU	1.10^{+10}	0.00	0.00	est.[28]
	KiBo_AG	1.10^{+10}	0.00	0.00	est.[28]
	Updated Aramco2.0	NI[b]			
	Glarborg	1.10^{+10}	0.00	0.00	est.[28]
CO + OH (+ M) ↔ HOCO (+ M)	KiBo_MU	$1.2.10^{+07}$7.2.10^{+25}	1.83−3.85	−2361550	ab initio[60]ab initio[60]
	KiBo_AG[a]	$2.6.10^{+20}$	−3.50	1309	mod.[61]
	Updated Aramco2.0[a]	$2.6.10^{+20}$	−3.50	1309	mod.[61]
	Glarborg[a]	$2.6.10^{+20}$	−3.50	1309	mod.[61]
OCHO + O_2 ↔ CO_2 + HO_2	KiBo_MU	$5.0.10^{+13}$	0.00	0.00	est.[28]
	KiBo_AG	$5.0.10^{+13}$	0.00	0.00	est.[28]
	Updated Aramco2.0	NI[b]			
	Glarborg	$5.0.10^{+13}$	0.00	0.00	est.[28]
	KiBo_AG	$4.6.10^{+12}$9.5.10^{+06}	0.002.00	−89−89	ab initio[58]ab initio[58]
	Updated Aramco2.0	$4.6.10^{+12}$9.5.10^{+06}	0.002.00	−89−89	ab initio[58]ab initio[58]
	Glarborg	$4.6.10^{+12}$9.5.10^{+06}	0.002.00	−89−89	ab initio[58]ab initio[58]

[a]Pressure-dependent reaction, rate coefficient at 1 atm. [b]NI: not included. [c]Units are cm^3, mol, s, cal, and K.

reactions such as CO + OH ↔ CO_2 + H, CO + OH ↔ HOCO, HOCO + M ↔ CO_2 + H + M, and HOCHO + OH ↔ OCHO + H_2O have a dominant promoting effect on the overall reactivity under the investigated conditions resulting from the generation of active H radical. The oxidation of CO to CO_2 through the reaction CO + OH ↔ CO_2 + H showed high sensitivity to the fuel flame, following the literature considering this reaction responsible for the main heat release step in several combustion systems[56] and the dominant route for CO_2 production.[57] Comparably, at φ = 0.8 and stoichiometric conditions, CO + OH ↔ CO_2 + H and HOCO + M ↔ CO_2 + H + M showed a strong positive sensitivity coefficient in KiBo_AG than KiBo_MU, while the opposite is true in the case of the CO + OH ↔ HOCO reaction. However, in rich flames, the CO + OH ↔ HOCO and HOCO + M ↔ CO_2 + H + M reactions show a relatively lower sensitivity coefficient in the case of KiBo_MU than KiBo_AG, whereas CO + OH ↔ CO_2 + H is equally sensitive to laminar burning velocity in both mechanisms.

On the other hand, in lean and rich flames using KiBo_MU, HOCO + H ↔ CO + H_2O, HOCHO + OH ↔ HOCO + H_2O, HOCO + O_2 ↔ CO_2 + H_2, HOCHO + H ↔ HOCO + H_2, HOCO + OH ↔ CO_2 + H_2O, and HOCO + H ↔ CO_2 + H_2 were orderly found to negatively affect the burning rate of formic acid oxidation, in which HOCO + H ↔ CO + H_2O had a strong hindering effect on the burning rate. Except for the last reaction (i.e., HOCO + H ↔ CO_2 + H_2), which is insensitive under stoichiometric conditions, all other reactions also show negative sensitivity to combustion rate under stoichiometric conditions. In the same way, using KiBo_AG, in lean, stoichiometric, and rich conditions, reactions having an obstructing effect on the laminar burning velocity are listed in order of their impact as HOCO + O_2 ↔ CO_2 + HO_2, HOCHO + OH ↔ HOCO + H_2O, HOCO + H ↔ CO + H_2O, and HOCO + O_2 ↔ CO_2 + HO_2, 2 HOCO ↔ HOCHO + CO_2, and HOCHO + OH ↔ HOCO + H_2O, respectively.

Under the investigated conditions, HOCO + H ↔ CO_2 + H_2, HOCHO + H ↔ HOCO + H_2, and HOCO + OH ↔ CO_2 + H_2O are insensitive to laminar burning rates in the case of KiBo_AG, but they are found to hinder the burning rate in the case of KiBo_MU. Likewise, 2 HOCO ↔ HOCHO + CO_2 is only sensitive in rich flame in the case of KiBo_AG. It is worth mentioning that this reaction was not included in KiBo_MU. Indeed, the procedure implemented for the realization of this mechanism considered only the H-abstraction by small radicals as primary reactions to limit the number of reactions. Furthermore, it is interesting to mention that in the case of KiBo_AG at φ = 0.8 and 1.0, all the sensitive reactions have similar sensitivity coefficient values, which was not the case for rich flame and KiBo_MU.

Overall, from flux analysis and sensitivity studies, it has been found that formic acid combustion is ruled by unimolecular decomposition, H-abstraction, and radical consumption reactions. The rate coefficients for the main unimolecular decomposition reactions of HOCHO incorporated in all the investigated mechanisms were taken from the study reported by Chang et al.,[25] whereas the H-abstraction reactions (i.e., via H, OH, HO_2, and O_2) were taken from the studies reported by Marshall and Glarborg[28] and Anglada.[26] Similarly, reaction rates of H-abstraction reactions of the intermediate radical HOCO (via OH, O_2, HO_2, and O) included in the investigated mechanisms were similar and taken from the same source.[27,58,59] Table 3 reports the kinetic coefficients and sources of reactions indicated by sensitivity analysis and flux diagram if missing or differing in any of the investigated mechanisms.

4. CONCLUSIONS

Given the rising concerns about the importance of formic acid chemistry in modern chemical societies and energy industries, the kinetic study of formic acid oxidation is very crucial. This study aims at characterizing the chemistry of oxygenated species, with specific reference to formic acid at low initial temperatures. To this aim, two different strategies resulting in kinetic models named KiBo_MU and KiBo_AG were implemented and compared. KiBo_MU contains 141 species and 453 reactions, whereas KiBo_AG comprises 90 species and 1047 reactions. The models were tested against validated models and experimental laminar burning velocity and jet-stirred data of formic acid available in the literature under a wide range of initial temperatures and equivalence ratios, showing excellent accuracy also concerning the existing mechanisms. Furthermore, the key sensitive reactions playing an important role in formic acid oxidation have been analyzed, and the reactions CO + OH ↔ HOCO, CO + OH ↔ CO_2 + H, HOCHO + OH ↔ OCHO + H_2O, and HOCO + M ↔ CO_2 + H + M were found to have a

https://doi.org/10.1021/acs.energyfuels.2c03249
Energy Fuels 2022, 36, 14382−14392

dominant promoting effect on laminar burning velocity. Similarly, from the jet-stirred study, decarboxylation reaction, hydrogen abstraction by HO_2 of HOCHO, and the abstraction reaction of HOCO radical by O_2 are found to be the key reactions affecting the consumption of HOCHO, which is consistent with the flux analysis study.

The agreement between experimental and numerical data confirms the robustness of the available thermochemical databases under the investigated conditions. Hence, the produced mechanisms can be intended as a paramount building block for the generation of detailed kinetic mechanisms for larger species, including biofuels. However, the validity of the mechanisms may suffer from a dearth of experimental data at high initial temperatures, partially related to the elevated corrosiveness of the investigated species. Hence, dedicated experimental campaigns properly designed to deal with the peculiar properties of the reactive system are strongly enviable.

■ ASSOCIATED CONTENT

Supporting Information

The Supporting Information is available free of charge at https://pubs.acs.org/doi/10.1021/acs.energyfuels.2c03249.

The kinetic mechanism manually updated in this work (KiBo_MU) (TXT)

The kinetic mechanism automatically generated in this work (KiBo_AG) (TXT)

■ AUTHOR INFORMATION

Corresponding Author

Gianmaria Pio − *Dipartimento di Ingegneria Civile, Chimica, Ambientale e dei Materiali, Università di Bologna, 40131 Bologna, IT, Italy;* orcid.org/0000-0002-0770-1710; Email: gianmaria.pio@unibo.it

Authors

Fekadu Mosisa Wako − *Dipartimento di Ingegneria Civile, Chimica, Ambientale e dei Materiali, Università di Bologna, 40131 Bologna, IT, Italy;* orcid.org/0000-0003-3928-0612

Ernesto Salzano − *Dipartimento di Ingegneria Civile, Chimica, Ambientale e dei Materiali, Università di Bologna, 40131 Bologna, IT, Italy;* orcid.org/0000-0002-3238-2491

Complete contact information is available at: https://pubs.acs.org/10.1021/acs.energyfuels.2c03249

Notes

The authors declare no competing financial interest.

■ REFERENCES

(1) Lawrence, J. E.; Koutrakis, P. Measurement of atmospheric formic and acetic acids: Methods evaluation and results from field studies. *Environ. Sci. Technol.* **1994**, *28*, 957−964.

(2) Chebbi, A.; Carlier, P. Carboxylic acids in the troposphere, occurrence, sources, and sinks: A review. *Atmos. Environ.* **1996**, *30*, 4233−4249.

(3) Zervas, E.; Montagne, X.; Lahaye, J. The influence of gasoline formulation on specific pollutant emissions. *J. Air Waste Manage. Assoc.* **1999**, *49*, 1304−1314.

(4) Zervas, E.; Montagne, X.; Lahaye, J. Emission of specific pollutants from a compression ignition engine. Influence of fuel hydrotreatment and fuel/air equivalence ratio. *Atmos. Environ.* **2001**, *35*, 1301−1306.

(5) Schauer, J. J.; Kleeman, M. J.; Cass, G. R.; Simoneit, B. R. T. Measurement of emissions from air pollution sources. 3. C1− C29 organic compounds from fireplace combustion of wood. *Environ. Sci. Technol.* **2001**, *35*, 1716−1728.

(6) Zervas, E.; Montagne, X.; Lahaye, J. C1− C5 organic acid emissions from an SI engine: Influence of fuel and air/fuel equivalence ratio. *Environ. Sci. Technol.* **2001**, *35*, 2746−2751.

(7) Biagini, E.; Barontini, F.; Tognotti, L. Devolatilization of biomass fuels and biomass components studied by TG/FTIR technique. *Ind. Eng. Chem. Res.* **2006**, *45*, 4486−4493.

(8) Zaras, A. M.; Szőri, M.; Thion, S.; Van Cauwenberghe, P.; Deguillaume, F.; Serinyel, Z.; Dayma, G.; Dagaut, P. A. Chemical Kinetic Investigation on Butyl Formate Oxidation: *Ab Initio* Calculations and Experiments in a Jet-Stirred Reactor. *Energy Fuels* **2017**, *31*, 6194−6205.

(9) Held, T. J.; Dryer, F. L. A comprehensive mechanism for methanol oxidation. *Int. J. Chem. Kinet.* **1998**, *30*, 805−830.

(10) Blades, A. T. The kinetics of the pyrolysis of ethyl and isopropyl formates and acetates. *Can. J. Chem.* **1954**, *32*, 366−372.

(11) Fischer, S. L.; Dryer, F. L.; Curran, H. J. The reaction kinetics of dimethyl ether. I: High-temperature pyrolysis and oxidation in flow reactors. *Int. J. Chem. Kinet.* **2000**, *32*, 713−740.

(12) Ansari, K. B.; Arora, J. S.; Chew, J. W.; Dauenhauer, P. J.; Mushrif, S. H. Fast pyrolysis of cellulose, hemicellulose, and lignin: Effect of operating temperature on bio-oil yield and composition and insights into the intrinsic pyrolysis chemistry. *Ind. Eng. Chem. Res.* **2019**, *58*, 15838−15852.

(13) Marinov, N. M. A detailed chemical kinetic model for high temperature ethanol oxidation. *Int. J. Chem. Kinet.* **1999**, *31*, 183−220.

(14) Christensen, M.; Konnov, A. A. Laminar burning velocity of acetic acid+ air flames. *Combust. Flame* **2016**, *170*, 12−29.

(15) Battin-Leclerc, F.; Konnov, A. A.; Jaffrezo, J.-L.; Legrand, M. To better understand the formation of short-chain acids in combustion systems. *Combust. Sci. Technol.* **2007**, *180*, 343−370.

(16) Eppinger, J. r.; Huang, K.-W. Formic acid as a hydrogen energy carrier. *ACS Energy Lett.* **2017**, *2*, 188−195.

(17) Sarathy, S. M.; Brequigny, P.; Katoch, A.; Elbaz, A. M.; Roberts, W. L.; Dibble, R. W.; Foucher, F. Laminar Burning Velocities and Kinetic Modeling of a Renewable E-Fuel: Formic Acid and Its Mixtures with $H_2$and CO_2. *Energy Fuels* **2020**, *34*, 7564−7572.

(18) Dyer, C. K.; Moseley, P. T.; Ogumi, Z.; Rand, D. A.; Scrosati, B. *Encyclopedia of electrochemical power sources*; Elsevier Science & Technology., 2009.

(19) Park, W.; Park, S.; Reitz, R. D.; Kurtz, E. The effect of oxygenated fuel properties on diesel spray combustion and soot formation. *Combust. Flame* **2017**, *180*, 276−283.

(20) Zervas, E. Formation of organic acids from propane, isooctane and toluene/isooctane flames. *Fuel* **2005**, *84*, 691−700.

(21) Yin, G.; Gao, Q.; Hu, E.; Xu, J.; Zhou, M.; Huang, Z. Experimental and kinetic study on laminar flame speeds of formic acid. *Combust. Flame* **2020**, *220*, 73−81.

(22) Osipova, K. N.; Sarathy, S. M.; Korobeinichev, O. P.; Shmakov, A. G. Laminar Burning Velocities of Formic Acid and Formic Acid/Hydrogen Flames: An Experimental and Modeling Study. *Energy Fuels* **2021**, *35*, 1760−1767.

(23) Bone, W. A.; Gardner, J. Comparative studies of the slow combustion of methane, methyl alcohol, formaldehyde, and formic acid. *Proc. R. Soc. London, Ser. A* **1936**, *154*, 297−328.

(24) Taylor, P. H.; Rahman, M. S.; Arif, M.; Dellinger, B.; Marshall, P. Kinetic and mechanistic studies of the reaction of hydroxyl radicals with acetaldehyde over an extended temperature range. In *Symposium (International) on Combustion*, 1996; Elsevier: Vol. *26*, pp. 497−504.

(25) Chang, J.-G.; Chen, H.-T.; Xu, S.; Lin, M.-C. Computational study on the kinetics and mechanisms for the unimolecular decomposition of formic and oxalic acids. *J. Phys. Chem. A* **2007**, *111*, 6789−6797.

(26) Anglada, J. M. Complex mechanism of the gas phase reaction between formic acid and hydroxyl radical. Proton coupled electron transfer versus radical hydrogen abstraction mechanisms. *J. Am. Chem. Soc.* **2004**, *126*, 9809−9820.

(27) Yu, H.-G.; Poggi, G.; Francisco, J. S.; Muckerman, J. T. Energetics and molecular dynamics of the reaction of HOCO with HO 2 radicals. *J. Chem. Phys.* **2008**, *129*, 214307.
(28) Marshall, P.; Glarborg, P. Ab initio and kinetic modeling studies of formic acid oxidation. *Proc. Combust. Inst.* **2015**, *35*, 153−160.
(29) de Wilde, E.; Van Tiggelen, A. Burning velocities in mixtures of methyl alcohol, formaldehyde or formic acid with oxygen. *Bull. Soc. Chim. Belg.* **1968**, *77*, 67−75.
(30) Burke, U.; Metcalfe, W. K.; Burke, S. M.; Heufer, K. A.; Dagaut, P.; Curran, H. J. A detailed chemical kinetic modeling, ignition delay time and jet-stirred reactor study of methanol oxidation. *Combust. Flame* **2016**, *165*, 125−136.
(31) Pio, G.; Palma, V.; Salzano, E. Comparison and validation of detailed kinetic models for the oxidation of light alkenes. *Ind. Eng. Chem. Res.* **2018**, *57*, 7130−7135.
(32) Kee, R. J.; Rupley, F. M.; Miller, J. A. *The Chemkin thermodynamic data base*; Sandia National Labs.: Livermore, CA (USA), 1990.
(33) Goldsmith, C. F.; Magoon, G. R.; Green, W. H. Database of small molecule thermochemistry for combustion. *J. Phys. Chem. A* **2012**, *116*, 9033−9057.
(34) Yaws, C. L. *Yaws' critical property data for chemical engineers and chemists*; Knovel, 2012.
(35) Goldsmith, C. F.; Green, W. H.; Klippenstein, S. J. Role of O2+ QOOH in low-temperature ignition of propane. 1. Temperature and pressure dependent rate coefficients. *J. Phys. Chem. A* **2012**, *116*, 3325−3346.
(36) West, R. H.; Allen, J. W.; Green, W. H. Abstract: Automatic Reaction Mechanism Generation with Group Additive Kinetics. *Indian J. Chem.* **2012**, *43* (), DOI: 10.1002/chin.201236258.
(37) Gao, C. W.; Allen, J. W.; Green, W. H.; West, R. H. Reaction Mechanism Generator: Automatic construction of chemical kinetic mechanisms. *Comput. Phys. Commun.* **2016**, *203*, 212−225.
(38) Susnow, R. G.; Dean, A. M.; Green, W. H.; Peczak, P.; Broadbelt, L. J. Rate-based construction of kinetic models for complex systems. *J. Phys. Chem. A* **1997**, *101*, 3731−3740.
(39) Dana, A. G.; Buesser, B.; Merchant, S. S.; Green, W. H. Automated reaction mechanism generation including nitrogen as a heteroatom. *Int. J. Chem. Kinet.* **2018**, *50*, 243−258.
(40) Smith, G.; Tao, Y.; Wang, H. *Foundational fuel chemistry model version 1.0 (FFCM-1)*; Stanford University *epub, accessed July* 2016, *26*, 2018.
(41) Burke, M. P.; Chaos, M.; Ju, Y.; Dryer, F. L.; Klippenstein, S. J. Comprehensive H_2/O_2 kinetic model for high-pressure combustion. *Int. J. Chem. Kinet.* **2012**, *44*, 444−474.
(42) Hashemi, H.; Christensen, J. M.; Gersen, S.; Levinsky, H.; Klippenstein, S. J.; Glarborg, P. High-pressure oxidation of methane. *Combust. Flame* **2016**, *172*, 349−364.
(43) Li, X.; Jasper, A. W.; Zádor, J.; Miller, J. A.; Klippenstein, S. J. Theoretical kinetics of O+ C2H4. *Proc. Combust. Inst.* **2017**, *36*, 219−227.
(44) Cohen, N.; Benson, S. W. Estimation of heats of formation of organic compounds by additivity methods. *Chem. Rev.* **1993**, *93*, 2419−2438.
(45) Khanshan, F. S. *Automatic generation of detailed kinetic models for complex chemical systems*; Northeastern University, 2016.
(46) Goodwin, D. G. An open-source, extensible software suite for CVD process simulation. *Chemical vapor deposition XVI and EUROCVD* **2003**, *14*, 2003−2008.
(47) Pio, G.; Carboni, M.; Salzano, E. Realistic aviation fuel chemistry in computational fluid dynamics. *Fuel* **2019**, *254*, 115676.
(48) Gao, X.; Yang, S.; Sun, W. A global pathway selection algorithm for the reduction of detailed chemical kinetic mechanisms. *Combust. Flame* **2016**, *167*, 238−247.
(49) Moffat, H. K.; Goodwin, D. G.; Speth, R. L. *Cantera: An object-oriented software toolkit for chemical kinetics, thermodynamics, and transport processes. Version 2.2. 1.*; Cantera Developers: Warrenville, IL 2017.
(50) Osipova, K. N.; Sarathy, S. M.; Korobeinichev, O. P.; Shmakov, A. G. Chemical structure of atmospheric pressure premixed laminar formic acid/hydrogen flames. *Proc. Combust. Inst.* **2021**, *38*, 2379−2386.
(51) Ranzi, E.; Frassoldati, A.; Grana, R.; Cuoci, A.; Faravelli, T.; Kelley, A. P.; Law, C. K. Hierarchical and comparative kinetic modeling of laminar flame speeds of hydrocarbon and oxygenated fuels. *Prog. Energy Combust. Sci.* **2012**, *38*, 468−501.
(52) Joshi, A. V.; Wang, H. Master equation modeling of wide range temperature and pressure dependence of CO+ $\vec{OH}$ products. *Int. J. Chem. Kinet.* **2006**, *38*, 57−73.
(53) Lavadera, M. L.; Konnov, A. A. Laminar burning velocities of methane+ formic acid+ air flames: Experimental and modeling study. *Combust. Flame* **2021**, *225*, 65−73.
(54) Yin, G.; Xu, J.; Hu, E.; Gao, Q.; Zhan, H.; Huang, Z. Experimental and kinetic study on the low temperature oxidation and pyrolysis of formic acid in a jet-stirred reactor. *Combust. Flame* **2021**, *223*, 77−87.
(55) Maharjan, S.; Elbaz, A. M.; Roberts, W. L. Investigation on the formic acid evaporation and ignition of formic acid/octanol blend at elevated temperature and pressure. *Fuel* **2022**, *313*, 122636.
(56) Miller, J. A.; Kee, R. J.; Westbrook, C. K. Chemical Kinetics and Combustion Modeling. *Annu. Rev. Phys. Chem.* **1990**, *41*, 345−387.
(57) Mohapatra, S.; Garnayak, S.; Lee, B. J.; Elbaz, A. M.; Roberts, W. L.; Dash, S. K.; Reddy, V. M. Numerical and chemical kinetic analysis to evaluate the effect of steam dilution and pressure on combustion of n-dodecane in a swirling flow environment. *Fuel* **2021**, *288*, 119710.
(58) Francisco, J. S.; Muckerman, J. T.; Yu, H.-G. HOCO radical chemistry. *Acc. Chem. Res.* **2010**, *43*, 1519−1526.
(59) Yu, H.-G.; Muckerman, J. T.; Francisco, J. S. Quantum force molecular dynamics study of the reaction of O atoms with HOCO. *J. Chem. Phys.* **2007**, *127*, No. 094302.
(60) Senosiain, J. P.; Musgrave, C. B.; Golden, D. M. Temperature and pressure dependence of the reaction of OH and CO: Master equation modeling on a high-level potential energy surface. *Int. J. Chem. Kinet.* **2003**, *35*, 464−474.
(61) Senosiain, J. P.; Klippenstein, S. J.; Miller, J. A. A complete statistical analysis of the reaction between OH and CO. *Proceedings of the combustion institute* **2005**, *30*, 945−953.